

Evaluating hypolimnetic diffusion parameters in thermally stratified lakes

Alon Rimmer,¹ Werner Eckert, and Aminadav Nishri

Israel Oceanographic & Limnological Research Ltd. Yigal Allon Kinneret Limnological Laboratory, P.O. Box 447, Migdal, 14950 Israel

Yehuda Agnon

Faculty of Civil and Environmental Engineering and Grand Water Research Institute (GWRI), Technion, Israel Institute of Technology, Haifa 32000, Israel

Abstract

The vertical transport of solutes in the anoxic hypolimnion of thermally stratified lakes can be described by a one-dimensional diffusion model. Using ammonium and dissolved methane as inert tracers, the model was solved, both analytically and numerically, for Lake Kinneret while taking into account sedimentary release, hypolimnetic transport, and the deepening of the thermocline depth. An average seasonal turbulent diffusion coefficient in the hypolimnion of $1.5 \pm 0.5 \text{ m}^2 \text{ d}^{-1}$ was confirmed independently by both tracers. In all cases, the modeled hypolimnetic distribution pattern was highly correlated with the actual measurements.

In thermally stratified lakes, the differentiation into a nutrient-enriched hypolimnion and a nutrient-depleted epilimnion is a common feature, and the vertical mixing between both layers affect geochemical and biological processes and, as such, the water quality. In the hypolimnion, horizontal transport is governed by advection (e.g., Marti and Imberger 2005). Vertical hypolimnetic transport is a result of diapycnal mixing events, which have to overcome the vertical density gradient and, therefore, is several orders of magnitude slower. Many models do not resolve these mixing events. Instead they are parameterized by averaging and are represented by a vertical diffusion coefficient. Literature values on the vertical diffusion coefficient (D_T) vary at large by up to four orders of magnitude (Table 1).

While the reported studies rely on indirect measurements and experiments to estimate the vertical diffusivity, we introduce an approach using natural tracers. Ideally, such a tracer should be constrained by the following features: being easy to measure, well-defined source and sink terms, and being inert to biogeochemical uptake. The hypolimnetic enrichment of solutes is a common feature among thermally stratified eutrophic lakes (Wetzel 1983). Among these are ammonium and dissolved methane, both of which are inert under anoxic conditions. Their distribution within the hypolimnion is governed by release and mixing processes, and their concentrations have been repeatedly shown to decrease from the lake bottom toward

the chemocline (Imboden et al. 1983; Bedard and Knowles 1991; Nishri et al. 2000). Similar was the total hypolimnetic content of both molecular species reported to increase linearly over time during the stratified period (Bedard and Knowles 1991). Both observations render NH_4^+ and CH_4 (diss) as ideal tracers for hypolimnetic transport processes.

In the present study, we introduce a one-dimensional model, aimed to evaluate the seasonal dynamics of both tracers in the hypolimnion of thermally stratified Lake Kinneret. With the model, we solve simultaneously for their release from the sediment–water interface (SWI), their vertical transport in the hypolimnion, and for the mixing at the thermocline, i.e., upper boundary of the hypolimnion. A major objective was to verify the vertical diffusion coefficient in the hypolimnion based on natural tracers.

Methodology

Study area—Lake Kinneret (LK) is a warm, monomictic freshwater lake located in the northern part of the Afro-Syrian Rift valley. The lake has a surface area of 168 km² (22 km long by 12 km wide) and a total volume of $4 \times 10^9 \text{ m}^3$ (Fig. 1). Average and maximum depths are 24 and 42 m, respectively. The Jordan River is the major inflow, while water pumped into the National Water Carrier constitutes the main outflow. Because maximum water input and exploitation occur in different seasons, the lake level fluctuates between 209 and 213 m below mean sea level. The lake is thermally stratified from April until December/January, with surface water temperatures ranging between 15°C in winter to 30°C in summer. During the summer months (May–August), it is strongly forced by daily westerly winds (e.g., Serruya 1975; Antenucci et al. 2000). The thermocline depth (Fig. 2) is initially (April) at 9–13 m, stabilizes during summer at 15–20 m, and begins to decline gradually in October until full mixis (late December–mid-January). The chemical stratification in the water column of LK conforms to a distinct seasonal pattern. During the time period of mixis (December–

¹ Corresponding author (alon@ocean.org.il).

Acknowledgments

This research was partly supported by grant from the G.I.F, the German-Israeli Foundation for Scientific Research and Development. We acknowledge the field technical and monitoring staff and the data base managers from Mekorot Watershed Unit (Israel), and the Kinneret Limnological Laboratory (Israel). We would like to thank Udi Wagner for his help with the numerical procedure, and Professor Johan Varekamp, and an anonymous reviewer for their helpful comments.

Table 1. Literature values on the vertical diffusion coefficient (D_T).

D_T	Method	Reference
0.173–8.64 m ² d ⁻¹	Review of estimates of basin averaged methods	Imberger and Patterson (1990)
0.008–0.086 m ² d ⁻¹	Tracer distribution and heat flux measurements	Goudsmit et al. (1997)
0.008–0.086 m ² d ⁻¹	Turbulent kinetic energy balance	Wüest et al. (2000)
1.7–3.5 m ² d ⁻¹	Tracer (phosphate)	Stiller (1974)
0.008–86.4 m ² d ⁻¹	High resolution temperature profiles	Yeates and Imberger (2003)
0.09–0.9 m ² d ⁻¹	Comparison of different methods	Imboden and Wüest (1995)

March), oxygen concentrations are high throughout the water column (Serruya 1978). With the onset of thermal stratification in April, hypolimnetic oxygen is gradually depleted (Fig. 2), followed by the accumulation of reduced solutes, such as sulfide, ammonium, and methane.

Theory

The governing equations—The temporal development of a vertical inert tracer distribution in the hypolimnion was illustrated in Fig. 3. It can be described by the one-dimensional diffusion equation,

$$\frac{\partial C}{\partial t} = S_c + \frac{\partial}{\partial z} \left(D_T \frac{\partial C}{\partial z} \right) = S_c + \frac{\partial D_T}{\partial z} \frac{\partial C}{\partial z} + D_T \frac{\partial^2 C}{\partial z^2} \quad (1)$$

where C represents the concentration of the tracer in the hypolimnion (g m⁻³); D_T is the vertical eddy diffusion coefficient (m² d⁻¹); S_c is the in situ production/consumption rate (g m⁻³ d⁻¹); t is the time (day), and z the vertical coordinate pointing upward, with $z = 0$ at the lake floor.

For solving Eq. 1, we made the following assumptions: (a) On a seasonal time scale, D_T can be treated as a vertical and temporal averaged constant for the mixing processes (Goudsmit et al. 1997). (b) Because the chosen tracers are inert under anoxic conditions and the hypolimnetic production is negligibly small (see results and discussion), $S_c \cong 0$. This assumption should be implemented with caution. In other lakes (for example, Lake Biwa in Japan, M. Kumagai unpubl. data), oxic conditions may continuously dominate the hypolimnion, and as such prevent ammonium accumulation.

With the above assumptions (a and b), Eq. 1 now simplifies to

$$\frac{\partial C}{\partial t} = D_T \frac{\partial^2 C}{\partial z^2} \quad (2)$$

The analysis proposed for Eq. 2 focuses on a one-dimensional vertical solution of the diffusion equation, and

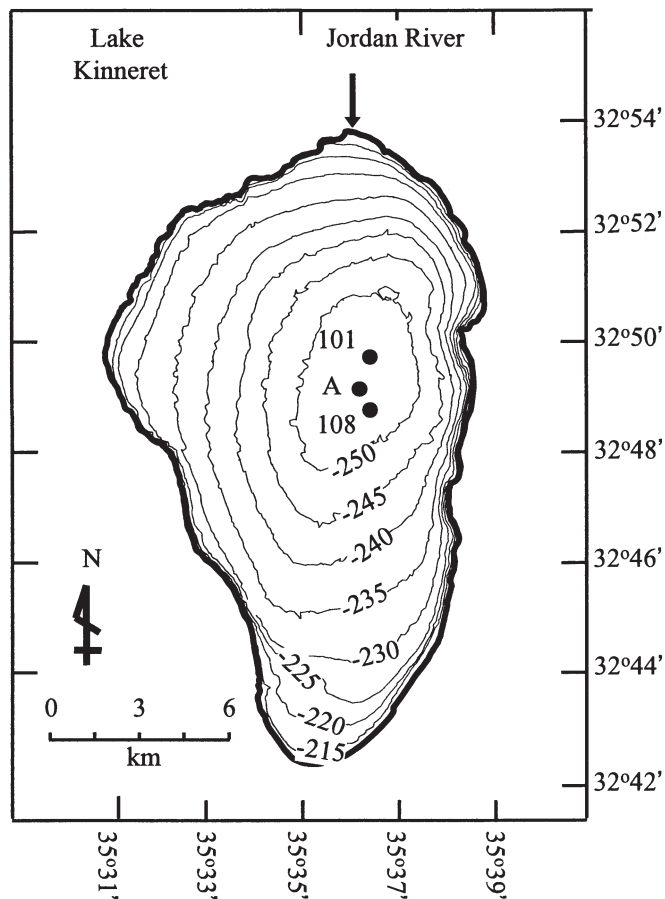


Fig. 1. Bathymetric map of Lake Kinneret, with the location of the monitoring stations at the lake's center.

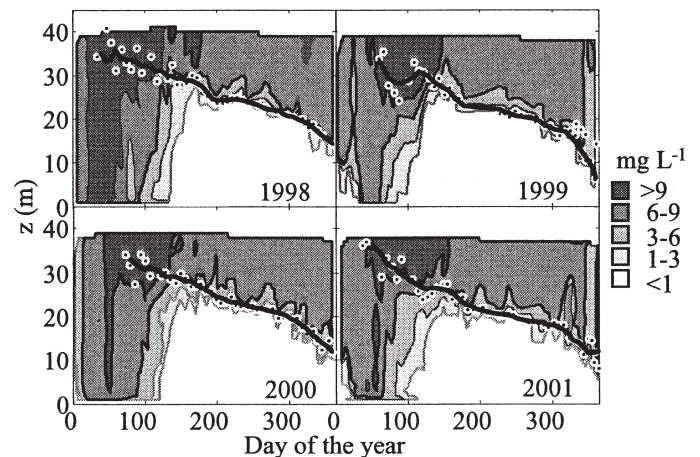


Fig. 2. Isopleth diagram of the seasonal variability of dissolved-oxygen concentrations (0–12 mg L⁻¹) in the water column of Lake Kinneret for the years 1998–2001. Black circles represent the thermocline depth calculated from weekly temperature profiles using the method of Rimmer et al. (2005); the solid line represents the smoothed thermocline used for the model.

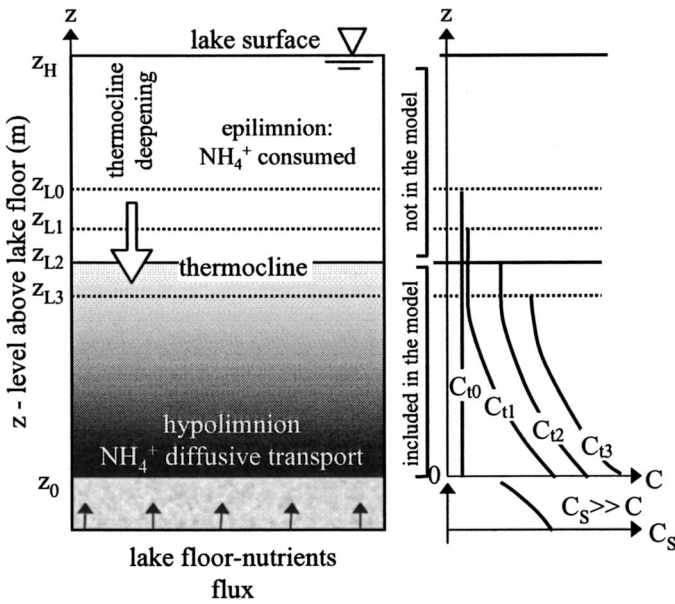


Fig. 3. Schematic representation of the proposed model setup. The water column is separated into two layers with z_0 the sediment–water interface, C_s represents the pore-water concentration, z_L is the vertical extension of the hypolimnion and $z_H - z_L$ that of the epilimnion. The z_{L_i} 's are vertical locations of the thermocline while it is deepening toward the end of the stratified period, and the C_{i_i} 's are the profiles of concentrations in the hypolimnion.

we are particularly interested in the characteristics of solutes that originate at the SWI.

Boundary conditions—If we define the tracer's inventory S in the hypolimnetic column as

$$S(t) = \int_{z=0}^{z=z_L} C(z, t) dz \quad (3)$$

where $z = z_0$ is the SWI and $z = z_L$ is the elevation of the thermocline, then the time change in the tracer's inventory is given by

$$\frac{dS(t)}{dt} \equiv \frac{\partial}{\partial t} \int_{z=z_0(t)}^{z=z_L(t)} C(z, t) dz = q(z_L, t) + q(0, t) \quad (4)$$

where q represents the inward Lagrangian fluxes of a tracer through the lower (Eq. 5) and upper (Eq. 6) boundaries of the hypolimnion, e.g., the SWI and the thermocline.

$$q(z, t) \equiv -D_T \frac{\partial C(z, t)}{\partial z} = A; \quad (z = 0, t > 0) \quad (5)$$

$$\begin{aligned} q(z, t) &\equiv D_T \frac{\partial C(z, t)}{\partial z} + C(z, t) \frac{dz}{dt} \\ &= C(z, t) \times v_{Th}; \quad (z = z_L, t > 0) \end{aligned} \quad (6)$$

$D_T \partial C / \partial z$ is the diffusive flux through the respective hypolimnetic boundary, and $C \partial z / \partial t$ is the solute flux associated with the speed of the thermocline deepening v_{Th} .

Our assumption to set the diffusion flux of NH_4^+ and CH_4 (diss) at the SWI in Eq. 5 constant is justified by long-term pore-water measurements of both solutes. During the stratified seasons (May–December) of the years 1998 until 2004, NH_4^+ concentrations in the uppermost sediment layer at the central lake station A varied between 4.2 and 6.2 mg N L⁻¹, and in the case of dissolved methane, the pore water was found to be CH_4 saturated (~ 25 ppm) at all times below a depth of 1–2 cm (Eckert unpubl. data). As such, the concentration gradient at the SWI was always greater than 4 mg N cm⁻¹ and 15 ppm CH_4 , supporting our postulation of seasonally constant release rates.

The postulation of a constant sedimentary flux is further justified by the findings of Berner (1980), who showed, for the case of ammonium, that under typical steady-state conditions, not only the ammonium concentration in the pore water, but also the gradient dC/dz at the water–sediment interface is constant in time.

The solute flux across the thermocline (Eq. 6) includes both mixing due to the erosion of the thermocline and the diffusive flux. Regarding the latter, vertical eddy diffusivity becomes nearly zero at the thermocline because the high-density gradient introduces a large restoring force that greatly inhibits vertical motion. This condition allows setting the term $D_T \partial C(z_L, t) / \partial z = 0$ (which is mathematically equivalent to setting $D_T = 0$ at $z = z_L$ in Eq. 6). This simplification is confirmed by the findings of Rimmer et al. (2005), who showed that the transport of solutes from the hypolimnion to the epilimnion in LK is quantitatively described by the mass transfer due to thermocline deepening.

Once the whole water column is mixed, both tracers are readily oxidized due to nitrification and microbial methane oxidation. As a result, the system is reset for the next accumulation period, with

$$C(z, t) = 0; \quad (z, t = 0) \quad (7)$$

The numerical solution—The governing Eq. 2 and the boundary conditions (Eqs. 5–7) were converted to finite differences explicit forward time-step formula as follows (see also Fig. 3):

$$\begin{aligned} C(z_j, t_{i+1}) &= C(z_j, t_i) + D_T \frac{\Delta t}{(\Delta z)^2} [C(z_{j+1}, t_i) \\ &\quad + C(z_{j-1}, t_i) - 2C(z_j, t_i)] \end{aligned} \quad (8)$$

where $i = 0, 1, 2, \dots, N_i$ and $j = 0, 1, 2, \dots, N_j$ are the time step and z elevations, respectively. The constant flux at $z = 0$ (Eq. 5) and the no diffusive flux boundary at $z = z_L$ (Eq. 6) were produced by

$$\begin{aligned} C(z_0, t_{i+1}) &= C(z_0, t_i) + \frac{\Delta t}{(\Delta z)^2} \\ &\quad \times [A \times \Delta z + D_T (C(z_1, t_i) - C(z_0, t_i))] \end{aligned} \quad (9)$$

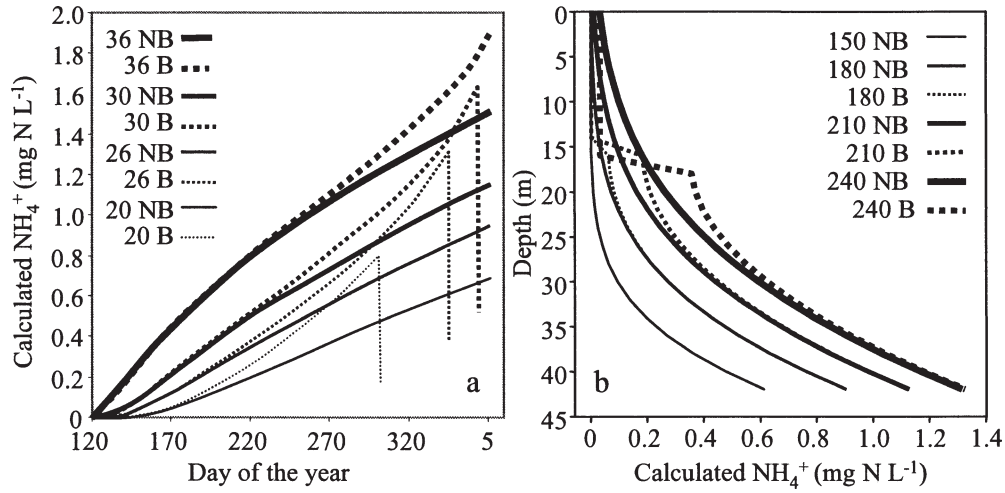


Fig. 4. Numerical solution of Eq. 2 with $A = 160 \text{ mg m}^{-2} \text{ d}^{-1}$, $D_T = 2 \text{ m}^2 \text{ d}^{-1}$, $z_H = 42 \text{ m}$, $\Delta z = 2 \text{ m}$, and $\Delta t = 1 \text{ d}$, subjected to two different upper boundary conditions. B (dotted lines) indicates the case when the upper boundary drops down and affects the tracer distribution (Eq. 6). NB (solid lines) indicates no effect of the upper boundary (Eq. 13). (a) Solution vs. time for 36, 30, 26, and 20 m depth; (b) solution vs. depth for 150, 180, 210, and 240 m ds.

$$C(z_L, t_{i+1}) = C(z_L, t_i) + D_T \frac{\Delta t}{(\Delta z)^2} \times [C(z_{L-1}, t_i) - C(z_L, t_i)] \quad (10)$$

The thermocline location for every timestep was interpolated from temperature profiles as described by Rimmer et al. (2005) to create the distinct series of (z_L, t_i) . The fluxes across the thermocline and the exchange of tracer between the hypolimnion and epilimnion were rephrased for the numeric scheme as follows:

$$q(z_L, t_i) = \begin{cases} C(z_L, t_i) \times i \times \Delta z; & i > 0 \\ 0; & i = 0 \end{cases} \quad (11)$$

Here, the flux that leaves the hypolimnion at any time step is a product of the concentration at the thermocline and the rate of displacement of z_L during a single time step, and i indicates the number of Δz units of the thermocline displacement. Mass balance of C in the epilimnion (which is not included in the model), was conducted in order to ensure the quality of the numerical scheme.

$$C(e, t_{i+1}) \times [z_H(t_{i+1}) - z_L(t_{i+1})] = C(z_L, t_i) \times \Delta z + C(e, t_i) \times [z_H(t_i) - z_L(t_i)] \quad (12)$$

Here, e represents the entire depth of the epilimnion and z_H is the elevation of the lake surface. Equation 12 is identical to the mass-balance equation proposed by Rimmer et al. (2005) and similar to the one by Varekamp (2003).

The goal of the simulation was to determine the mean seasonal values of both A and D_T . They were optimized over a range of D_T and A values that best fit a set of simulated results to measured concentration profiles. The numerical solution process was as follows:

1. The season was selected (1998, 1999, 2000, etc.); initial concentration was set to $C = 0$, and Δz was set at 0.4 m for the entire season.
2. Initial realistic ranges of D_T ($0.5\text{--}2.5 \text{ m}^2 \text{ d}^{-1}$) and A ($50\text{--}250 \text{ mg m}^{-2} \text{ d}^{-1}$) were defined.
3. For each D_T , the criterion for the scheme's stability was calculated as $\Delta t < (0.5 \times \Delta z^2) / D_T$ (Botha and Pinder 1983) and the numerical solution (Eqs. 8–12) was calculated for the entire range of the A values.
4. Modeled C profiles for the entire season were compared with measured concentrations of ammonium (or methane) in the hypolimnion. For each comparison, a value of correlation (r^2) was calculated.
5. Best-fit D_T and A parameters were defined for each season from the best value of r^2 .

The analytical solutions—One advantage of using analytical rather than numerical solutions is in the procedure of extracting the optimal parameters. The disadvantage in our case is that the problem of diffusion with moving boundary falls into the category of Stefan-problems that generally cannot be solved analytically. This obstacle can be circumvented by solving the problem for either a limited time or for limited depth.

Limited time: At the beginning of stratification, the diffusive distribution of materials released from the lake floor is affected only by the lower boundary condition (Eq. 5). The upper boundary (Eq. 6) will come into play once the tracer has reached the thermocline, e.g., $C(z_L, t_i) > 0$. By replacing Eq. 6 with a different type of upper boundary condition,

$$C = 0; (z = L, t > 0); \quad L \gg z_L \quad (13)$$

where L is an arbitrarily chosen, very large height (i.e., 1,000 m) throughout the stratification period, we ensure

that the solution for short time periods will not be affected by the upper boundary. Using the hypolimnetic ammonium accumulation as an example, Figure 4 shows the numerical solution of Eq. 2 for both scenarios. The dotted line represents the first case (with Eq. 6) and the solid line represents the second case (with Eq. 13). Both accumulation patterns follow initially the same trend. The time point of diversion increased with the size of the selected t and z values. We therefore propose that, for small t and z , Eq. 2, subject to the boundary conditions Eqs. 5, 7, and 13, may be solved analytically using separation of variables (e.g., Pinchover and Rubinstein 2005):

$$C(z, t) = (z - L)A^* + \frac{8A^*L}{\pi^2} \times \sum_{n=1}^{\infty} \frac{\exp\left(-D_T(2n-1)^2\pi^2(t-\tau)/(2L)^2\right)}{(2n-1)^2} \times \cos\left(\frac{2n-1}{2}\frac{\pi z}{L}\right) \quad (14)$$

$$A^* = -A/D_T; \quad n = 1, 2, 3, \dots, \infty$$

Here, τ is the day when ammonium or methane begins to accumulate in the hypolimnion and n is an arbitrary variable over which we sum the terms on the right-hand side of Eq. 14.

Limited depth: Alternatively, we can replace the boundary condition on the moving thermocline, by prescribing the measured value $C(b, t) = f(t)$ at a constant level b , for as long as b is located within the hypolimnion. For this problem, we write the solution once more using separation of variables (e.g., Pinchover and Rubinstein 2005). We first approximate $f(t)$ as a sum of exponential functions of time (e.g., via least-squares approximation):

$$f\{t\} = \sum_{n=1}^N a_n [1 - \exp(D_T\alpha_n^2 t/b^2)] \quad (15)$$

The values α_n are chosen so that the series describes well the variation of $f(t)$. We define

$$C_1(z, t) = (z - b)A^* + \sum_{n=1}^N a_n \times [1 - \exp(D_T\beta_n^2 t/b^2)] \cosh(\alpha_n z/b) / \cosh(\beta_n) \quad (16)$$

Then C_1 satisfies the boundary conditions for C at $z = 0$ and at $z = b$. In order to satisfy the initial condition, $C(z_0) = 0$, we add the function

$$C_2(z, t) = \sum_{m=1}^M b_m \exp\left(-D_T(m-1/2)^2\pi^2 t/b^2\right) \times \cos((m-1/2)\pi z/b) \quad (17)$$

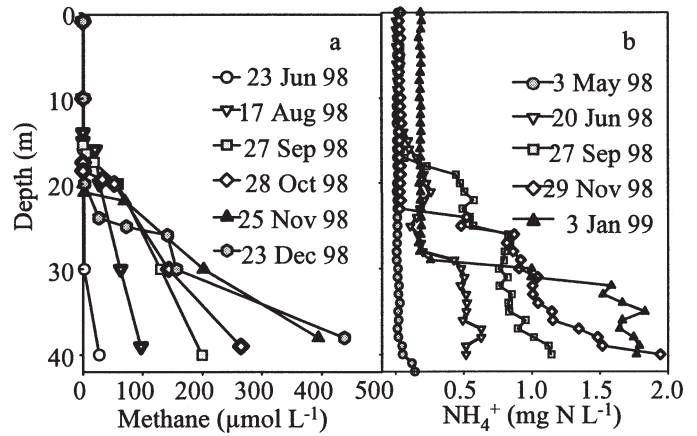


Fig. 5. (a) Methane and (b) ammonium concentration profiles measured in the water column of Lake Kinneret during the stratification period of 1998.

Using the orthogonality of $\cos((m-1/2)\pi z/b)$ over $0 < z < 2b$, we find

$$b_n = \frac{2bA^*}{(m-1/2)^2\pi^2} + (-1)^n \times \sum_{n=1}^N \frac{2\beta_n^2 a_n}{\pi(m-1/2)[(m-1/2)^2\pi^2 + \beta_n^2]} \quad (18)$$

Making

$$C(z, t) = C_1(z, t) + C_2(z, t) \quad (19)$$

the required solution.

With the solutions in Eqs. 14 or 19, we can use several standard functions in MATLAB to find both the best-fit values of A^* , D_T , and τ , and the 95% confidence interval for each season.

Monitoring data

The proposed analysis was tested in detail on long-term data sets of (1) lake level, measured on a daily basis by the Israeli Hydrological Service. (2) Temperature profiles from the central monitoring stations of LK (sta. A; ~42 m depth; Fig. 1) provided by the LK database (LKDB). Temperature profiles were measured on a weekly basis using STD-12 Plus (Applied Microsystems Ltd.) with an error of $\pm 0.005^\circ\text{C}$. (3) Detailed biweekly to monthly ammonium concentration profiles from the central lake stations (A, 101, and 108; Fig. 1). Data for the period 1998–2001 were provided by the MEKOROT water company. The ammonium assay used is that of the indophenol technique (APHA 2001). Dissolved methane in station A was measured biweekly in water samples, sampled at 5-m intervals plus three thermocline samples (1-m interval) using gas-chromatographic headspace analysis on water samples (after Schmidt and Conrad 1993). Typical methane and ammonium concentration profiles measured during the 1998 lake cycle are presented in Fig. 5a,b, respectively, confirming the nearly linear increase of both

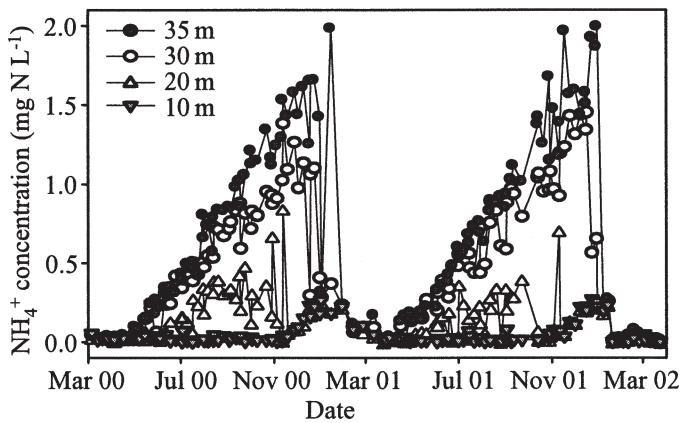


Fig. 6. Time series of the ammonium concentration in the water column of Lake Kinneret at four fixed depths (35, 30, 20, and 10 m) from March 2000 to March 2002.

solutes from the SWI to the thermocline. The accumulation pattern of the hypolimnetic ammonium concentration during two consecutive stratified periods (35- and 30-m series in Fig. 6) substantiates our constant-release-rate assumption.

Results and discussion

Numerical solution—The results of the numerical solution were tested against measured profiles of NH_4^+ and CH_4 (diss) for the period 01 May–31 Dec of the years 1998–2001 and 1999–2000, respectively. The contour plot of the cumulative square error between the predicted and measured NH_4^+ in the hypolimnion during the year 2001 (Fig. 7) shows that the optimum values of D_T and A were defined well in the range of 0.5–2.5 $\text{m}^2 \text{d}^{-1}$ and 50–250 $\text{mg} \text{m}^{-2} \text{d}^{-1}$, respectively. The contours also demon-

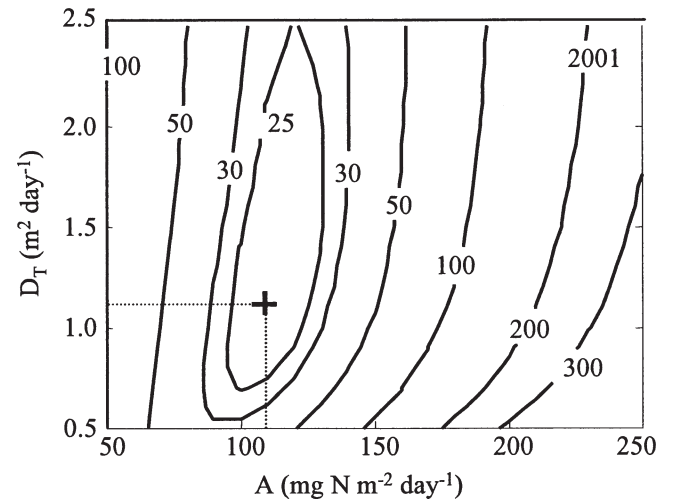


Fig. 7. Contour plot and best fit (+) of the cumulative square error between predicted and calculated NH_4^+ concentrations in the hypolimnion of Lake Kinneret during 2001 for D_T and A values ranging between 0.5 and 2.5 $\text{m}^2 \text{d}^{-1}$ and 50 and 250 $\text{mg} \text{N} \text{m}^{-2} \text{d}^{-1}$, respectively.

strate that the proposed diffusion mechanism has a unique solution for these two parameters. The correlation factor between measured and calculated concentrations using the best-fit parameters for each season was always large ($r^2 > 0.79$, Table 2). Calculated and measured profiles of hypolimnetic ammonium concentrations are compared in Fig. 8 for the 1998–1999 stratification periods. While both data sets are generally in good agreement, discrepancies occur mainly near the SWI during early stratification (Fig. 8, profiles of 30 August 1998 and 27 June 1999). We assume that, during the months May–August, the water profile is typically influenced by the relatively strong westerly winds, which, in turn,

Table 2. Optimal parameters A , D_T and τ ; 5% error; and r^2 as they were calculated using the analytical solution (Eq. 14) for the period 01 May to 31 Dec in station 108, and 01 May to 30 Sep in stations 108, 101, and A.

Year	Station	A	σ_A	D_T	σ_{D_T}	τ	σ_τ	r^2
		($\text{g} \text{m}^{-2} \text{d}^{-1}$)		($\text{m}^2 \text{d}^{-1}$)		(day of the year)		
01 May to 31 Dec								
1998	108	150	18	2.53	0.45	126	4	0.81
1999	108	166	19	1.50	0.26	123	6	0.88
2000	108	153	14	2.64	0.35	129	3	0.87
2001	108	137	15	1.74	0.29	122	6	0.89
01 May to 30 Sep								
1998	108	143	17	4.08	0.67	122	3	0.85
1999	108	165	22	3.23	0.65	115	4	0.90
2000	108	155	15	3.79	0.51	127	2	0.87
2001	108	165	18	3.54	0.59	123	4	0.89
1998	101	133	32	5.48	1.91	123	3	0.74
1999	101	174	30	4.04	1.07	116	4	0.89
2000	101	199	22	6.22	1.07	132	3	0.88
2001	101	200	32	5.39	1.37	125	5	0.82
1998	A	133	23	4.62	1.17	123	5	0.90
1999	A	118	19	1.61	0.39	104	10	0.94
2000	A	134	18	2.53	0.50	125	5	0.90
2001	A	135	20	2.50	0.57	120	7	0.89

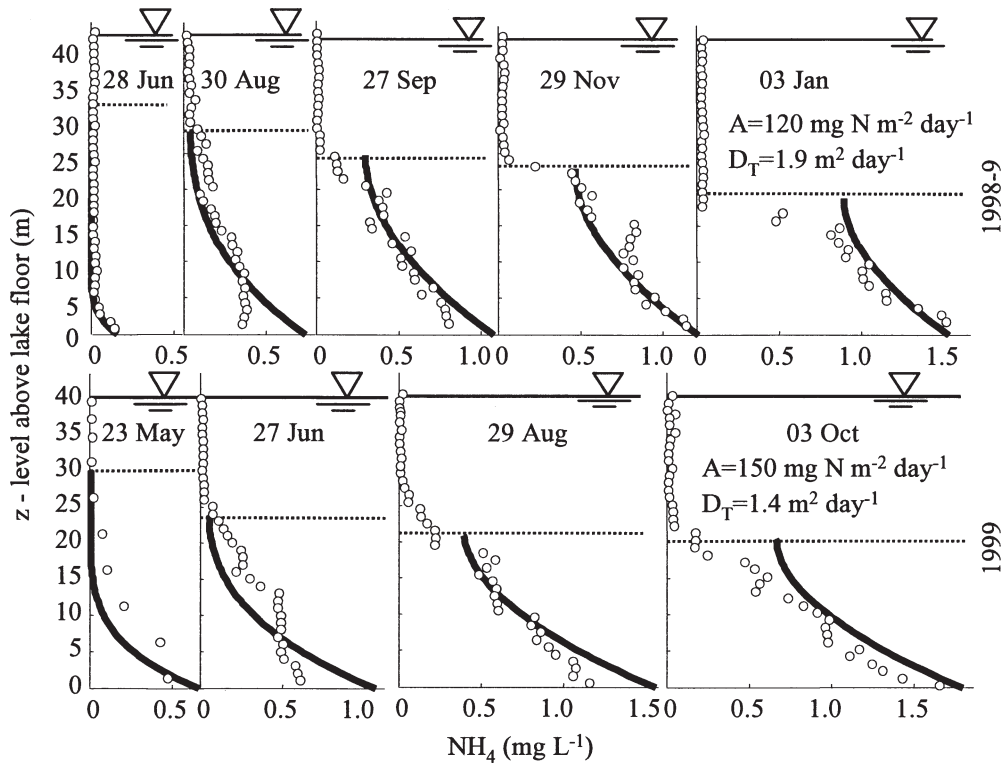


Fig. 8. Comparison between calculated and measured ammonium profiles during the 1998–1999 stratified periods.

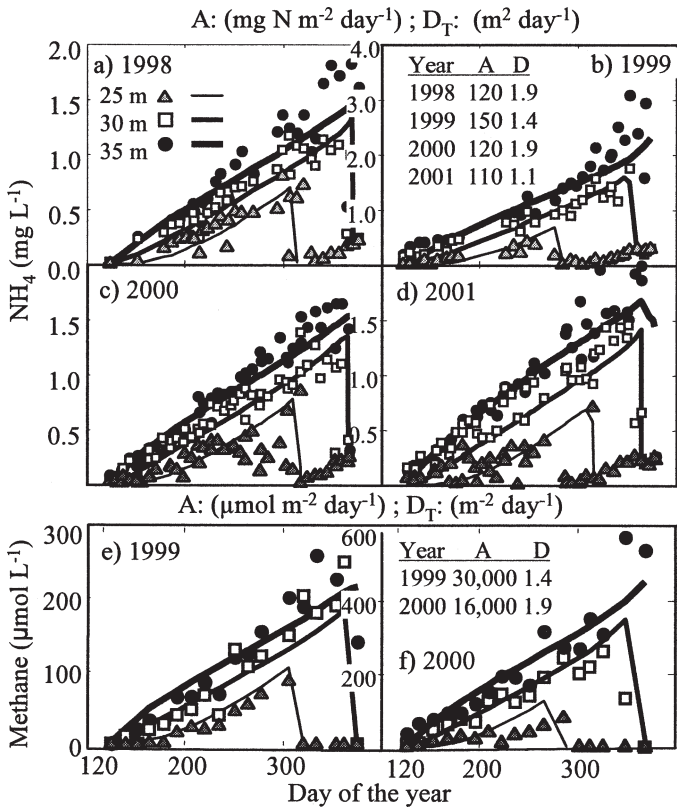


Fig. 9. Measured (markers) and calculated (lines) time series of (a–d) hypolimnetic NH₄⁺ and (e, f) methane concentrations at three representative depths (35, 30, and 25 m) during the seasons 1998–2000.

increase the diffusion coefficient in the benthic boundary layer, an effect that is ignored by the proposed constant D_T model. A second discrepancy can be observed near the thermocline boundary, especially at the end of the stratification period (Fig. 8, profiles of 03 Jan 1999 and 03 Oct 1999). This difference is due to the fact that the model was developed for a two-layer system, e.g., hypolimnion and epilimnion, while ignoring the existence of a metalimnion. However, in view of our general goal to model hypolimnetic transport processes, the error induced by this simplification is minor.

We are aware of the possibility of secondary sources of the chosen tracers within the hypolimnion, i.e., NH₄⁺ generation during the mineralization of sinking particulate organic matter or dissolution of gaseous methane from sedimentary gas ebullition events. In the course of our investigations, and after tests of solutions with $S_c > 0$, we arrived at the conclusion that the influence of these secondary sources is negligible because, in this case, we would anticipate considerable differences between measured profiles and the model results.

A second means to verify the model output data is to follow time series of hypolimnetic NH₄⁺ and CH₄ (diss) concentrations at fixed depths (Fig. 9a–f). The resulting accumulation pattern approaches a nearly linear increase at all occasions. The seasonal best-fit values of D_T and A are listed for both solutes in Fig. 9b,f, respectively. It is important to note that D_T values for the 1999 and 2000 seasons were nearly identical for both solutes while being calculated independently. This finding emphasizes D_T as being an actual physical property of the

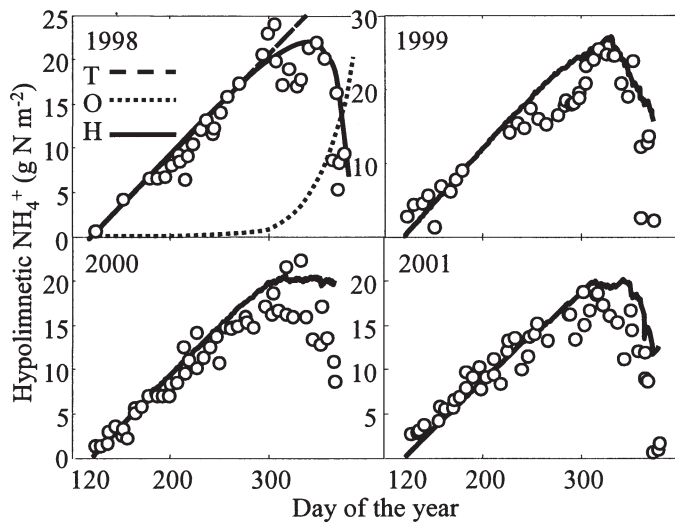


Fig. 10. Time change in the hypolimnetic ammonium inventory integrated from measured (circles) and modeled (lines) profiles during the 1998–2001 stratified periods. For 1998, the modeled inventory (H; solid line) is presented as the difference between the theoretical sedimentary input (T; dashed line) and outflow (O; dotted line) due to thermocline erosion.

hypolimnetic profile, which characterizes the seasonal process.

We further integrated in situ and model data, in order to follow seasonal changes in the hypolimnetic ammonium inventory (Fig. 10). According to the model, the linear increase observed from the beginning of May until the end of October is explained by the constant inflow of released ammonium from the SWI (Eq. 5), while the outflows (Eq. 6) are negligible because of the small concentration at the thermocline plane and the slow thermocline erosion. The gradual decrease during November and December is explained by the increased erosion of the thermocline, while at the same time the concentration of the tracer at the thermocline is significantly larger than at the beginning of the stratification period. The product $C(z_L, t)dz_L/dt$, attributed to the outflow from the hypolimnion, keeps increasing, and during December, it becomes larger than the inflows from the lake floor. At this time, the hypolimnetic ammonium inventory starts to decrease until the whole water column is mixed, accompanied by the fast depletion of NH_4^+ by aerobic nitrifying bacteria.

Analytical solution—The optimal parameters A , D_T , and τ were calculated for stations A, 108, and 101 (Table 2) using the analytical solution (Eq. 14). First, it was shown that, by taking into account all the measured profiles in station 108 between 01 May and 31 December, the optimal results of the analytical solution were similar to those of the numerical analysis. However, because the analytical solution is valid only for the first half of the stratification period and for large depth (Fig. 4), we calculated the optimal parameters only for the period 01 May to 30 September (~150 d, Table 2). The conclusions from this comparison are: (a) The proposed analysis results in similar

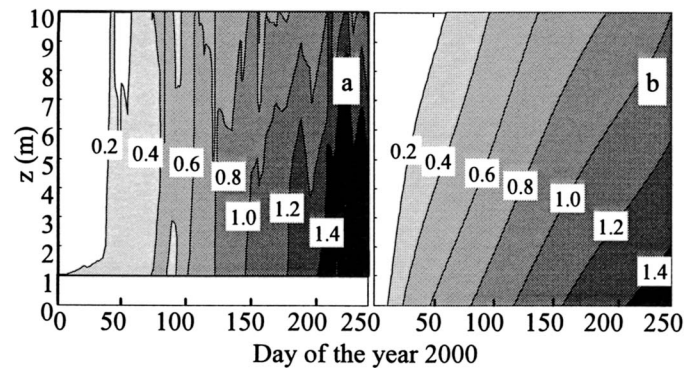


Fig. 11. The NH_4^+ distribution in $0 < z < 10$ m during the stratification period of the year 2000. (a) Contour plot based on the NH_4^+ measurements. (b) Contour plots based on the NH_4^+ prediction of the diffusion model (Eq. 19) with $A = 120 \text{ mg N m}^{-2} \text{ d}^{-1}$ and $D_T = 1.9 \text{ m}^2 \text{ d}^{-1}$.

optimal parameters and similar deviations for all three stations and therefore represents well the vertical transport processes in the entire area of the center of the lake. (b) There is a two times larger optimal D_T if we take into account the first half of the stratification compared with the entire period. It probably reflects the increased diffusion coefficient of the benthic boundary layer (BBL) during the months May–August, as was shown also in Fig. 8.

The results of the second analytical solution (Eq. 19) are demonstrated in Fig. 11, for the NH_4^+ distribution in $0 < z < 10$ m during the stratification period of the year 2000. We compared between the contours, which were produced by the NH_4^+ measurements, and those that were created by the prediction of the diffusion model. The prediction was based on the measurements of NH_4^+ in one single depth (~35 m) after they were applied to form the top boundary condition (Eq. 15), and on the constants $A = 120 \text{ mg m}^{-2} \text{ d}^{-1}$ and $D_T = 1.9 \text{ m}^2 \text{ d}^{-1}$ for the year 2000.

The proposed model approach, based on natural tracer distribution, was applied successfully to investigate the parameters that control the mechanism of solute transport in the hypolimnion. We showed one numerical and two analytical methods to calculate A and D_T .

Overall, the comparison between modeled and measured profiles reveals that the entire seasonal process can be described reasonably well using only two constants. The observed deviations reflect the limitations of the proposed model when applied to short time scales, such as a single measured profile or to a single depth during long-term measurements. The results of the one-dimensional model provide a systematic approach and better understanding of the changes in nutrients inventories, which is based on the history of the measured data.

An advantage of the proposed model and calibration is its potential usage to increase the certainty of the measured nutrient inventories and their change in time. The fact that the sedimentary release and hypolimnetic transport of an inert tracer can be sufficiently characterized by two constants is expected to be extremely useful when dealing with nonconservative solutes, such as phosphate or

dissolved organic carbon, that form similar steep gradients across the SWI. With D_T being readily accessible from the inert tracer and A being a function of the concentration gradient across the SWI, the difference between measured and modeled inventories should correspond to the sink term affecting the investigated solute.

The results from our study point out some challenging questions for future research. One addresses the interannual variability found regarding the driving parameters of our model: A and D_T . So far, we have tried in vain to link the observed fluctuations to annual changes in biogeochemical, hydrodynamic, and meteorological master variables. It will be further important to compare the D_T values from this research with basin-scale vertical diffusion calculated from temperature and salinity measurements.

References

- AMERICAN PUBLIC HEALTH ASSOCIATION (APHA). 2001. Standard methods for the examination of water and wastewater, 19th ed. American Public Health Association.
- ANTENUCCI, J., J. IMBERGER, AND A. SAGGIO. 2000. Seasonal evolution of the basin-scale internal wave field in a large stratified lake. *Limnol. Oceanogr.* **45**(7): 1621–1638.
- BÉDARD, C., AND R. KNOWLES. 1991. Hypolimnetic O_2 consumption, denitrification, and methanogenesis in thermally stratified lake. *Can. J. Fish. Aquat. Sci.* **48**: 1048–1054.
- BERNER, R. A. 1980. Early diagenesis, a theoretical approach. Princeton Univ. Press.
- BOTHA, J. F., AND G. F. PINDER. 1983. Fundamental concepts in the numerical solution of differential equations. John Wiley & Sons.
- ECKERT, W., J. IMBERGER, AND A. SAGGIO. 2002. Biogeochemical evolution in response to physical forcing in the water column of a warm monomictic lake. *Biogeochemistry* **61**: 291–307.
- GOUDSMIT, G.-H., F. PEETERS, M. GLOOR, AND A. WÜEST. 1997. Boundary versus internal diapycnal mixing in stratified natural waters. *J. Geophys. Res.* **102**(C13): 27903–27914.
- IMBERGER, J., AND J. PATTERSON. 1990. Physical limnology, p. 303–475. *In* T. Wu [ed.], *Advances in applied mechanics*, V. 27. Academic Press.
- IMBODEN, D. M., U. LEMMIN, T. JOLLER, AND M. SCHURTER. 1983. Mixing processes in lakes: Mechanisms and ecological relevance. *Schweiz. Z. Hydrol.* **45**: 11–44.
- , AND A. WÜEST. 1995. Mixing mechanisms in lakes, p. 83–138. *In* A. Lerman, D. M. Imboden and J. R. Gat [eds.], *Physics and chemistry of lakes*. Springer Verlag.
- MARTI, C. L., AND J. IMBERGER. 2005. The dynamic behavior of the benthic boundary layer in a thermally stratified lake, p. 225–232. *In* J. H. W. Lee and K. M. Lam [eds.], *Environmental hydraulics*, V. 1, *Proceedings of the 4th International Symposium on Environmental Hydraulics*, Hong Kong.
- NISHRI, A., J. IMBERGER, W. ECKERT, I. OSTROVOSKY, AND J. GEIFMAN. 2000. The physical regime and the respective biogeochemical processes in lower water mass of Lake Kinneret. *Limnol. Oceanogr.* **45**: 972–981.
- PINCHOVER, Y., AND J. RUBINSTEIN. 2005. An introduction to partial differential equations. Cambridge Univ. Press.
- RIMMER, A., Y. AOTA, M. KUMAGAI, AND W. ECKERT. 2005. Chemical stratification in thermally stratified lakes: A chloride mass balance model. *Limnol. Oceanogr.* **50**: 147–157.
- SCHMIDT, U., AND R. CONRAD. 1993. Hydrogen, carbon monoxide, and methane dynamics in Lake Constance. *Limnol. Oceanogr.* **38**: 1214–1226.
- SERRUYA, C. 1978. Water chemistry, p. 185–204. *In* C. Serruya [ed.], *Lake Kinneret*. Dr. W. Junk Publishers.
- SERRUYA, S. 1975. Wind, water temperature and motions in Lake Kinneret: General pattern. *Verh. Internat. Verein. Limnol.* **19**: 73–87.
- STILLER, M. 1974. Rates of transport and sedimentation in Lake Kinneret. Ph.D. thesis, The Weizmann Institute of Science, Rehovot, Israel.
- VAREKAMP, J. C. 2003. Lake contamination models for evolution towards steady state. *J. of Limnology* **62**(suppl.1): 67–72.
- WETZEL, R. G. 1983. *Limnology*. Saunders College Publishing.
- WÜEST, A., G. PIEPKE, AND D. C. VAN SENDEN. 2000. Turbulent kinetic energy balance as a tool for estimating vertical diffusivity in wind-forced stratified waters. *Limnol. Oceanogr.* **45**: 1388–1400.
- YEATES, P. S., AND J. IMBERGER. 2003. Pseudo two-dimensional simulations of internal and boundary fluxes in stratified lakes and reservoirs. *Intl. J. River Basin Manage* **1**: 297–319.

Received: 24 July 2005

Accepted: 5 January 2006

Amended: 24 January 2006